Communications in Applied and Industrial Mathematics,
ISSN 2038-0909, e-438
DOI: 10.1685/journal.caim.438

Energetic BEM-FEM coupling for wave propagation in layered media

Alessandra Aimi, Mauro Diligenti, Chiara Guardasoni, Stefano Panizzi

Dipartimento di Matematica e Informatica,
Università degli Studi di Parma, Italy
{*alessandra.aimi,mauro.diligenti,chiara.guardasoni,stefano.panizzi*}*@unipr.it*

Communicated by Giorgio Fotia

Abstract

Starting from a recently developed energetic space-time weak formulation of boundary integral equations related to wave propagation problems defined on single and multi domains, a coupling algorithm is presented, which allows a flexible use of finite and boundary element methods as local discretization techniques, in order to efficiently treat bounded or unbounded multilayered media. Partial differential equations associated to boundary integral equations will be weakly reformulated by the energetic approach and a particular emphasis will be given to theoretical and experimental analysis of the stability of the proposed method. First numerical results on wave propagation model problems related to 1D elastodynamics will be presented and discussed.

Keywords: `multilayered media, non-overlapping domain decomposition, energetic BEM-FEM coupling, 1D elastodynamics.`

AMS subject classification: `65N38, 65N30.`

1. Introduction.

Time-dependent problems that are frequently modeled by hyperbolic partial differential equations can be dealt with the boundary integral equations (BIEs) method. The transformation of the differential problem to a BIE follows the same well-known method for elliptic boundary value problems. For the discretization phase Boundary Element Methods (BEMs) are successfully applied in seismology, in particular for the study of the soil-structure interaction, in acoustic and in the analysis of the electromagnetic scattering (see e.g. [1–3]), taking advantage of dimensionality reduction and of the implicit enforcement of radiation conditions at infinity.
When one deals with regions having different material properties (e.g. layered soils, [4,5]) or even different physics (e.g. in solid-fluid coupling [6] or wave-soil-structure interaction [7]) domain decomposition is needed.
In this framework, BEM is nowadays understood to be complementary rather than concurrent to FEM.

Received on November 19th, 2012. Accepted on February 19th, 2013. Published on February 28th, 2013.

The boundary element method, also when formulated directly in the space-time domain, has attracted particular interest for:

- its high accuracy;
- the simplicity of imposing the interface conditions in problems defined on multi-domains: the continuity and compatibility conditions that have to be satisfied on the interface respectively by the primal unknown function and its derivative can be simply incorporated because they both appear directly in the boundary integral formulation;
- the implicit fulfillment of the infinity radiation conditions;
- the low cost of discretization when problems are defined over unbounded domains and the classical numerical methods (finite difference, finite element) cannot efficiently determine the solution having to insert artificial boundaries and consequently non-reflective conditions in order to try to significantly reduce spurious reflections of the wave propagating from the fictitious boundary towards the interior of the domain.

The use of BIEs and BEMs, however, is complex and not particularly efficient in presence of non-linearities localized in small parts of the domain. In this case, the classical differential models and numerical techniques, such as the finite difference method (FDM) and finite element method (FEM) help to efficiently deal with the nonlinear part of the problem, but require, in general, a fine discretization of the entire domain with a significant increase in computational cost, even if, when using fully unstructured grids, local mesh refinement is in principle feasible, at least in absence of strong inhomogeneities. Anyway, in this context, BEM and FEM methods for the approximation of boundary integral equations systems and systems of partial differential equations are complementary and a suitable coupling of these two techniques can take advantage of what both offer.
In the last decades, contributions to BEM-FEM coupling, in the context of hyperbolic problems, started to appear [8–11], especially analyzing stability issues.
In this work, starting from a recently developed energetic space-time weak formulation of BIEs related to wave propagation problems defined on single and multi domains (see in particular [12,13] and references therein), a coupling algorithm is presented, which allows a flexible use of FEM and BEM as local discretization techniques, in order to efficiently treat bounded or unbounded multilayered media. Partial differential equations associated to BIEs will be weakly reformulated by the energetic approach and a particular emphasis will be given to theoretical and experimental analysis of the

DOI: 10.1685/journal.caim.438

stability of the proposed method.
The paper is structured as follows: in Sections 2 and 3 the model problem and its energetic weak formulation are introduced; Section 4 is dedicated to the Galerkin BEM-FEM discretization phase; in Section 5 we obtain theoretical stability results using energy arguments. At last, in Section 6, several numerical results are presented and discussed.

2. The model problem.

The model problem here considered is the elastodynamic one, i.e. the propagation of stress waves in elastic media during a bounded time interval of analysis $(0, T)$. We will refer to the one-dimensional case which describes the propagation of displacement and traction fields along a weightless rod, when we impose an initial configuration different from that one of statical equilibrium, under small displacements hypothesis.
The rod under consideration can be represented by a structured 3D body, with a dimension much larger than the remaining ones: the length L along the x-direction. For this reason its geometry is describable by a line, the axial line of the rod, which passes through the barycenters of all transversal sections, while displacements and traction are referred to the axial coordinates of the bar.
The homogeneous linear-elastic material constituting the rod follows Hooke's law and no flexural moment is considered.
This model can be extended to one-dimensional wave propagation analysis in layered media as it will be described in the following.
The rod of length L is supposed to be constituted by two portions Ω_1, Ω_2 of length L_1, $L_2 = L - L_1$, respectively, made up by different materials with Young's modulus E_1, E_2, mass density ρ_1, ρ_2 and section area A_1 and A_2, respectively. As a consequence, the scalar wave propagation velocities in the two sub-domains Ω_i, i.e. $c_i = \sqrt{E_i/\rho_i}$, are allowed to be different.
We want to study the wave propagation problem with assigned conditions of mixed type (Dirichlet-Neumann) at the end-points of the rod. Hence, having denoted with $u_i(x,t)$ the longitudinal displacement, which is a function of space and time, and with $p_i(x,t) := E_i\, A_i\, \frac{\partial u_i}{\partial \mathbf{n}_x}(x,t)$ the traction, depending on a unitary (outward) normal vector with respect to the transversal section of the rod, therefore directed along the x-axis, i.e. $\mathbf{n}_x = (n_x\ 0\ 0)^\top$, and on $E_i A_i$, which represents the axial stiffness of the i-th part of the rod, considering a local reference system for each portion so that $\Omega_i = (0, L_i)$,

we want to solve the differential model problem:

$$(1)\quad \frac{\partial^2 u_i(x,t)}{\partial x^2} - \frac{\ddot{u}_i(x,t)}{c_i^2} = f_i(x,t), \qquad x \in \Omega_i,\ t \in (0,T), \quad i = 1,2,$$

$$(2)\quad u_i(x,0) = \dot{u}_i(x,0) = 0, \qquad x \in \Omega_i, \quad i = 1,2,$$

$$(3)\quad u_1(0,t) = \bar{u}_1(t), \quad p_2(L_2,t) = \bar{p}_2(t),\ t \in (0,T),$$

where overhead dots indicate derivatives with respect to time and $\bar{u}_1(t)$, $\bar{p}_2(t)$ are given functions, the assigned PDE right-hand sides $f_1(x,t) \equiv 0$ and $f_2(x,t)$, such that in local reference system $f_2(0,t) = 0$, are suitably connected and continuity and equilibrium conditions for the solutions are imposed at the interface between the two materials, i.e.:

$$(4)\quad u_1(L_1,t) = u_2(0,t) =: u_2^I(t), \qquad p_1(L_1,t) = -p_2(0,t) =: p_1^I(t).$$

The unknown functions u_i are understood in a weak sense, i.e. $u_i \in H^1((0,T);H^1(\Omega_i))$. Since the goal of this work is to approximate u_1 using a BEM approach and u_2 using a FEM technique, in order to obtain a boundary integral reformulation of the problem (1)–(3) in the first portion of the rod, we have to use Love's representation formula (the analogue in the dynamical case of the Somigliana identity for linear elastostatic), which depends on the fundamental solution of the hyperbolic equation (1). This fundamental solution corresponds to the displacements field generated in an unbounded rod by an impulsive load applied in a point ξ at the time instant τ, i.e. the solution of the differential problem

$$(5)\quad \frac{\partial^2 u_1(x,t)}{\partial x^2} - \frac{\ddot{u}_1(x,t)}{c_1^2} = -\frac{1}{E_1\,A_1}\,\delta(x-\xi)\,\delta(t-\tau), \quad x \in \mathbb{R},\ t > 0,$$

where δ is the Dirac distribution, and reads, having set $r = |x-\xi|$:

$$(6)\quad G_{uu}(x,\xi;t-\tau) = \frac{c_1}{2\,E_1\,A_1}\,H(t-\tau)\,H(c_1(t-\tau)-r),$$

where $H(t)$ is the Heaviside step function which assures the causality of the wave. The function (6) is known in literature as the first Kelvin solution. Multiplying the partial differential equation in (1) by $E_1A_1\,G_{uu}(x,\xi;t-\tau)$, integrating in space and time and using the integration by parts technique, one obtains the following Love's representation formula for the solution of (1)–(3), for $x \in \Omega_1$ and $t \in (0,T)$:

$$(7)\quad u_1(x,t) = \sum_{\xi=0,L_1} G_{uu}(x,\xi;t) * p_1(\xi,t) - \sum_{\xi=0,L_1} G_{up}(x,\xi;t) * u_1(\xi,t)\,,$$

DOI: 10.1685/journal.caim.438

where the asterisk denotes the time convolution product and $G_{up}(x,\xi;t)$ is the so called Gebbia first fundamental solution, given by:

(8)
$$G_{up}(x,\xi;t-\tau) = E_1 A_1 \frac{\partial G_{uu}}{\partial \mathbf{n}_\xi}(x,\xi;t-\tau) = \frac{c_1}{2} H(t-\tau) \frac{\partial H}{\partial \xi}(c_1(t-\tau)-r)\, n_\xi \,.$$

At this stage, it is clear that if we want to recover the solution of (1)–(3) in Ω_1, we have to know the time history of tractions in $x = 0$ and of displacements and traction in $x = L_1$, i.e. $p_1(0,t)$ and $u_1(L_1,t), p_1(L_1,t)$. With a limiting procedure in (7), for x tending to the boundary of Ω_1, we obtain a first BIE of the form:

$$(9) \quad u_1(x,t) = \sum_{\xi=0,L_1} G_{uu}(x,\xi;t) * p_1(\xi,t) - \sum_{\xi=0,L_1} G_{up}(x,\xi;t) * u_1(\xi,t),$$

for $x \in \{0, L_1\}$, $t \in (0,T)$.

The BIE (9) is generally used to solve wave problem with Dirichlet boundary conditions, but can be used in presence of mixed boundary conditions, too. Anyway, in this latter case, remembering the definition of $p_1(x,t)$, from (9) one can obtain a second BIE, of the form:

$$(10) \quad p_1(x,t) = \sum_{\xi=0,L_1} G_{pu}(x,\xi;t) * p_1(\xi,t) - \sum_{\xi=0,L_1} G_{pp}(x,\xi;t) * u_1(\xi,t),$$

for $x \in \{0, L_1\}$, $t \in (0,T)$.

In the BIE (10) we find the second Kelvin fundamental solution:

(11)
$$G_{pu}(x,\xi;t-\tau) = E_1 A_1 \frac{\partial G_{uu}}{\partial \mathbf{n}_x}(x,\xi;t-\tau) = \frac{c_1}{2} H(t-\tau) \frac{\partial H}{\partial x}(c_1(t-\tau)-r)\, n_x \,,$$

which represents the stress field generated by an impulsive load applied to the rod, and the derivative of Gebbia fundamental solution, i.e.:

$$(12) \quad G_{pp}(x,\xi;t-\tau) = E_1 A_1 \frac{\partial G_{up}}{\partial \mathbf{n}_x}(x,\xi;t-\tau)$$
$$= \frac{E_1 A_1 c_1}{2} H(t-\tau) \frac{\partial H}{\partial x\, \partial \xi}(c_1(t-\tau)-r)\, n_\xi\, n_x \,.$$

Of course, derivatives in (8), (11) and (12) have to be understood in a distributional sense.

For what concerns the boundary integral reformulation of the problem (1)–(3) in Ω_1, we will consider the BIE (9) in $x = 0$ and $x = L_1$, and the

second BIE (10) in $x = L_1$. Using the explicit expression of the kernels G_{uu}, G_{up}, G_{pu}, G_{pp} and the boundary datum in $x = 0$, one obtains, after an integration by parts involving the kernel G_{pp} and some straightforward calculations, the following integro-differential equation system, for $t \in (0, T)$,

$$
(13)\quad \begin{cases} \dfrac{c_1}{E_1A_1}\displaystyle\int_0^t p_1^0(\tau)\,\mathrm{d}\tau + \dfrac{c_1}{E_1A_1}\int_0^{t-L_1/c_1} p_1^{L_1}(\tau)\,\mathrm{d}\tau + u_1^{L_1}(t-\dfrac{L_1}{c_1}) = \bar{u}_1(t) \\ \dfrac{c_1}{E_1A_1}\displaystyle\int_0^{t-L_1/c_1} p_1^0(\tau)\,\mathrm{d}\tau + \dfrac{c_1}{E_1A_1}\int_0^t p_1^{L_1}(\tau)\,\mathrm{d}\tau - u_1^{L_1}(t) = -\bar{u}_1(t-\dfrac{L_1}{c_1}) \\ p_1^0(t-\dfrac{L_1}{c_1}) + p_1^{L_1}(t) - \dfrac{E_1A_1}{c_1}\,\dot{u}_1^{L_1}(t) = -\dfrac{E_1A_1}{c_1}\,\dot{\bar{u}}_1(t-\dfrac{L_1}{c_1}) \end{cases}
$$

in the unknown time functions $p_1^0(t) := p_1(0,t) \in H^0(0,T)$, $u_1^{L_1}(t) := u_1(L_1,t) \in H^1(0,T)$, $p_1^{L_1}(t) := p_1(L_1,t) \in H^0(0,T)$ respectively. Of course, this problem has to be coupled with (1)–(3) specified for Ω_2, under the coupling conditions (4) at the interface.

3. Energetic weak formulation for the coupling.

Let us observe that for the hyperbolic wave problem (1)–(3) related to Ω_1, the positive energy at the final time instant T can be expressed as:

$$
(14)\quad \begin{aligned} \mathcal{E}_{\Omega_1}(u_1,T) &:= \frac{1}{2}\int_{\Omega_1}\Big[\Big(\frac{\dot{u}_1(x,T)}{c_1}\Big)^2 + \Big(\frac{\partial u_1(x,T)}{\partial x}\Big)^2\Big]\,\mathrm{d}x \\ &= \frac{1}{E_1A_1}\int_0^T \sum_{x=0,L_1} \dot{u}_1(x,t)\,p_1(x,t)\,\mathrm{d}t \;\geq 0. \end{aligned}
$$

This expression is obtained multiplying the differential equation by $\dot{u}_1$ and integrating by parts in time and space over $(0,T)\times\Omega_1$, and leads to the so-called energetic weak formulations of the BIEs system. In fact, BIEs of type (9) will be differentiated with respect to time before being projected onto the space $H^0(0,T)$, while equations of type (10) will be projected onto the space of time derivatives of functions belonging to $H^1(0,T)$.
Having indicated with $<\cdot,\cdot>$ the standard scalar product in $H^0(0,T)$, the energetic weak form of system (13) is finally

(15)

$$
\begin{cases} \frac{c_1}{E_1A_1} < q_1^0(t), p_1^0(t) + p_1^{L_1}(t-\frac{L_1}{c_1}) + \frac{E_1A_1}{c_1}\dot{u}_1^{L_1}(t-\frac{L_1}{c_1}) > = < q_1^0(t), \dot{\bar{u}}_1(t) > \\ \frac{c_1}{E_1A_1} < q_1^{L_1}(t), p_1^0(t-\frac{L_1}{c_1}) + p_1^{L_1}(t) - \frac{E_1A_1}{c_1}\dot{u}_1^{L_1}(t) > = - < q_1^{L_1}(t), \dot{\bar{u}}_1(t-\frac{L_1}{c_1}) > \\ < \dot{v}_1^{L_1}(t), p_1^0(t-\frac{L_1}{c_1}) + p_1^{L_1}(t) - \frac{E_1A_1}{c_1}\dot{u}_1^{L_1}(t) > = -\frac{E_1A_1}{c_1} < \dot{v}_1^{L_1}(t), \dot{\bar{u}}_1(t-\frac{L_1}{c_1}) > \end{cases} ,
$$

DOI: 10.1685/journal.caim.438

where $q_1^0(t), q_1^{L_1}(t) \in H^0(0,T)$, $v_1^{L_1}(t) \in H^1(0,T)$.

For the energetic weak formulation in Ω_2, let us multiply the differential equation (1) for the time derivative of test functions $v_2(x,t) \in H^1((0,T);H^1(\Omega_2))$ and integrate by parts in space obtaining, after a multiplication by the coefficient $2E_2A_2$:

$$-\mathcal{A}(v_2,u_2) + 2 < \dot{v}_2^0(t), p_2^0(t) >= \mathcal{F}(v_2) - 2 < \dot{v}_2^{L_2}(t), \bar{p}_2(t) > , \tag{16}$$

where

$$\mathcal{A}(v_2,u_2) := 2E_2A_2 \int_0^T \int_{\Omega_2} \Big[\frac{\partial \dot{v}_2}{\partial x}(x,t) \frac{\partial u_2}{\partial x}(x,t) + \frac{1}{c_2^2} \dot{v}_2(x,t) \ddot{u}_2(x,t) \Big] \, dx \, dt \tag{17}$$

and

$$\mathcal{F}(v_2) := 2E_2A_2 \int_0^T \int_{\Omega_2} \dot{v}_2(x,t) f_2(x,t) \, dx \, dt \, . \tag{18}$$

Now, remembering (4), using the further coupling condition and definitions at interface for test functions

$$v_1^{L_1}(t) = v_2^0(t) =: v_2^I(t) \, , \quad q_1^{L_1}(t) =: q_1^I(t) \tag{19}$$

and combining this equation with the third weak BIE, we finally obtain the following energetic weak formulation of the coupled problem:

$$\begin{cases} \frac{c_1}{E_1A_1} < q_1^0(t), p_1^0(t) + p_1^I(t - \frac{L_1}{c_1}) + \frac{E_1A_1}{c_1} \dot{u}_2^I(t - \frac{L_1}{c_1}) >=< q_1^0(t), \dot{\bar{u}}_1(t) > \\ \frac{c_1}{E_1A_1} < q_1^I(t), p_1^0(t - \frac{L_1}{c_1}) + p_1^I(t) - \frac{E_1A_1}{c_1} \dot{u}_2^I(t) >= - < q_1^I(t), \dot{\bar{u}}_1(t - \frac{L_1}{c_1}) > \\ < \dot{v}_2^I(t), p_1^0(t - \frac{L_1}{c_1}) - p_1^I(t) - \frac{E_1A_1}{c_1} \dot{u}_2^I(t) > -\mathcal{A}(v_2,u_2) = \mathcal{F}(v_2) \\ \qquad\qquad - \frac{E_1A_1}{c_1} < \dot{v}_2^I(t), \dot{\bar{u}}_1(t - \frac{L_1}{c_1}) > -2 < \dot{v}_2^{L_2}(t, \bar{p}_2(t) > \end{cases} . \tag{20}$$

4. Galerkin BEM-FEM discretization.

For time discretization we consider a uniform decomposition of the time interval $[0,T]$ with time step $\Delta t = T/N_{\Delta t}$, $N_{\Delta t} \in \mathbb{N}^+$, generated by the $N_{\Delta t} + 1$ time-knots

$$t_k = k \, \Delta t, \quad k = 0, \cdots, N_{\Delta t} \, ,$$

and we choose temporally piecewise constant shape functions for the approximation of p and piecewise linear shape functions for the approximation

of u, although higher degree shape functions can be used. Note that, for this particular choice, temporal shape functions, for $k = 0, \cdots, N_{\Delta t} - 1$, will be defined as

$$\tilde{\psi}_k(t) = H(t - t_k) - H(t - t_{k+1}) \tag{21}$$

for the approximation of $p_1^0(t)$ and $p_1^I(t)$, or as

$$\psi_k(t) = R(t - t_k) - R(t - t_{k+1}), \tag{22}$$

for the approximation of the temporal part of $u_2(x,t)$, where $R(t - t_k) = \frac{t - t_k}{\Delta t} H(t - t_k)$ is the ramp function. Note that with this choice one has $\dot{\psi}_k(t) = \dfrac{1}{\Delta t} \tilde{\psi}_k(t)$.
On the second portion of the rod, we consider a mesh $\mathcal{T}_{\Delta x} = \{e_1, \cdots, e_{N_{\Delta x}}\}$ constituted by elements e_i such that $length(e_i) \leq \Delta x$, equipped by piecewise linear (hat) basis functions $\varphi_j(x)$, $j = 1, \cdots, N_{\Delta x} + 1$, although, even in this case, higher degree shape functions can be chosen.
With the above choices, the approximate solutions $\tilde{p}_1^0(t)$, $\tilde{p}_1^I(t)$ and $\tilde{u}_2(t)$ of the problem at hand will be expressed as

$$\tilde{p}_1^0(t) = \sum_{k=0}^{N_{\Delta t}-1} \alpha_k^0 \, \tilde{\psi}_k(t)\,, \qquad \tilde{p}_1^I(t) = \sum_{k=0}^{N_{\Delta t}-1} \alpha_k^I \, \tilde{\psi}_k(t)\,,$$

and

$$\tilde{u}_2(x,t) = \sum_{k=0}^{N_{\Delta t}-1} \sum_{j=1}^{N_{\Delta x}+1} \beta_{kj} \, \psi_k(t) \, \varphi_j(x).$$

The Galerkin BEM-FEM discretization coming from energetic weak formulation (20) produces the linear system

$$M \, \mathbf{x} = \mathbf{y}\,, \tag{23}$$

where matrix M has a block lower triangular Toeplitz structure, since its elements depend on the difference $t_h - t_k$ and in particular they vanish if $t_h < t_k$. Each block has dimension $N_{\Delta x} + 3$. If we denote by $M^{(\ell)}$ the block obtained when $t_h - t_k = \ell \, \Delta t$, $\ell = 0, \ldots, N_{\Delta t} - 1$, the linear system can be written as

(24)

$$\begin{pmatrix} M^{(0)} & 0 & 0 & \cdots & 0 \\ M^{(1)} & M^{(0)} & 0 & \cdots & 0 \\ M^{(2)} & M^{(1)} & M^{(0)} & \cdots & 0 \\ \cdots & \cdots & \cdots & \cdots & 0 \\ M^{(N_{\Delta t}-1)} & M^{(N_{\Delta t}-2)} & \cdots & M^{(1)} & M^{(0)} \end{pmatrix} \begin{pmatrix} \mathbf{x}^{(0)} \\ \mathbf{x}^{(1)} \\ \mathbf{x}^{(2)} \\ \vdots \\ \mathbf{x}^{(N_{\Delta t}-1)} \end{pmatrix} = \begin{pmatrix} \mathbf{y}^{(0)} \\ \mathbf{y}^{(1)} \\ \mathbf{y}^{(2)} \\ \vdots \\ \mathbf{y}^{(N_{\Delta t}-1)} \end{pmatrix}$$

DOI: 10.1685/journal.caim.438

where

$$\mathbf{x}^{(\ell)} = \left(x_j^{(\ell)}\right) , \quad \mathbf{y}^{(\ell)} = \left(y_j^{(\ell)}\right) , \quad \ell = 0, \ldots, N_{\Delta t} - 1; \; j = 1, \ldots, N_{\Delta x} + 3.$$

Note that each block $M^{(\ell)}$ is symmetric, highly sparse and it has a block sub-structure of the type

$$M^{(\ell)} = \begin{bmatrix} M_{BEM}^{(\ell)} & M_{BEM,I}^{(\ell)} & 0 \\ M_{I,BEM}^{(\ell)} & M_{I}^{(\ell)} & M_{I,FEM}^{(\ell)} \\ 0 & M_{FEM,I}^{(\ell)} & M_{FEM}^{(\ell)} \end{bmatrix} \tag{25}$$

where diagonal sub-blocks have dimensions, respectively, $1, 2, N_{\Delta x}$. Further, the unknowns are organized as follows

$$\mathbf{x}^{(\ell)} = \left(\alpha_\ell^0, \alpha_\ell^I, \beta_{\ell 1}, \cdots, \beta_{\ell N_{\Delta x}+1}\right)^\top .$$

The solution of (24) is obtained with a block forward substitution, i.e. at every time instant $t_\ell = (\ell + 1)\,\Delta t$, $\ell = 0, \cdots, N_{\Delta t} - 1$, one computes

$$\mathbf{z}^{(\ell)} = \mathbf{y}^{(\ell)} - \sum_{j=1}^{\ell} M^{(j)} \mathbf{x}^{(\ell - j)}$$

and then solves the reduced linear system:

$$M^{(0)} \mathbf{x}^{(\ell)} = \mathbf{z}^{(\ell)} . \tag{26}$$

Procedure (26) is a time-marching technique, where the only matrix to be inverted is the non-singular block $M^{(0)}$; all the other blocks are used to update at every time step the right-hand side. Owing to this procedure we can construct and store only the blocks $M^{(0)}, \cdots, M^{(N_{\Delta t}-1)}$. Note also that, due to the simplicity of the considered 1D model, the elements of the blocks $M^{(\ell)}$ have been evaluated analytically.

5. Energy estimates.

In order to simplify the notation in the theoretical analysis of the proposed technique, let us slightly change the model problem considering a geometric configuration of the rod which anyway is more important in the applications because it better justifies the use of coupling FEM with BEM. In fact, let us now suppose to consider an unbounded subdomain Ω_1 and that a Sommerfeld radiation condition is satisfied by displacement u_1 at infinity. Let us further consider trivial boundary condition also for the

bounded portion Ω_2, i.e. $\bar{p}_2 \equiv 0$. The above coupled energetic weak formulation (20) reads, in this case:

$$(27) \qquad \begin{cases} \frac{c_1}{E_1 A_1} < q_1^I(t), p_1^I(t) > - < q_1^I(t), \dot{u}_2^I(t) >= 0 \\ \\ < \dot{v}_2^I(t), p_1^I(t) > + \frac{E_1 A_1}{c_1} < \dot{v}_2^I(t), \dot{u}_2^I(t) > + \mathcal{A}(v_2, u_2) = -\mathcal{F}(v_2) \end{cases} .$$

Summing up the two weak equations in the unknowns $p_1^I(t)$ and $u_2(x,t)$, $x \in \Omega_2$, considering $q_1^I(t) = p_1^I(t)$ and $v_2(x,t) = u_2(x,t)$, the following relation for the energy holds:

$$(28) \qquad \frac{c_1}{E_1 A_1} |p_1^I|^2_{H^0(0,T)} + \frac{E_1 A_1}{c_1} |\dot{u}_2^I|^2_{H^0(0,T)} + 2E_2 A_2 \mathcal{E}_{\Omega_2}(u_2, T) = -\mathcal{F}(u_2)\,,$$

or, equivalently, remembering (14) specified for the present model,

$$(29) \qquad 2E_1 A_1 \mathcal{E}_{\Omega_1}(u_1, T) + 2E_2 A_2 \mathcal{E}_{\Omega_2}(u_2, T) = -\mathcal{F}(u_2)\,,$$

from which we can easily deduce a-priori stability estimates for regular solutions.
For what concerns energy estimates for the numerical scheme, having set:

$$(30) \qquad p_k^I := p_1(I, t_k), \quad u_k^I := u_2(I, t_k), \quad u_k := u_2(x, t_k)\,,$$

using the discretization described above and integrating only in time, the approximation of the previous system of weak equations (27) can be written in the following way:

$$(31) \qquad \begin{cases} \frac{c_1}{E_1 A_1} p_k^I - \frac{u_{k+1}^I - u_k^I}{\Delta t} = 0 \\ \\ \varphi(I) p_k^I + \frac{E_1 A_1}{c_1} \varphi(I) \frac{u_{k+1}^I - u_k^I}{\Delta t} + \frac{2E_2 A_2}{c_2^2} \left(\varphi, \frac{u_{k+1} - 2u_k + u_{k-1}}{\Delta t^2}\right) \\ \qquad\qquad + E_2 A_2\, a(\varphi, u_{k+1} + u_k) = 2E_2 A_2\, (\varphi, F_k) \end{cases}$$

where

$$(32) \qquad (\cdot,\cdot) := (\cdot,\cdot)_{L^2(\Omega_2)}, \quad a(\varphi, u) := \left(\frac{\partial \varphi}{\partial x}, \frac{\partial u}{\partial x}\right), \quad F_k(x) := \frac{1}{\Delta t} \int_{t_k}^{t_{k+1}} -f_2(x,t)\, dt$$

or equivalently

$$(33) \qquad \begin{cases} \frac{c_1 \Delta t}{E_1 A_1 E_2 A_2} p_k^I - \frac{1}{E_2 A_2} (u_{k+1}^I - u_k^I) = 0 \\ \\ \frac{1}{E_2 A_2} \varphi(I) p_k^I + \frac{E_1 A_1}{E_2 A_2 c_1} \varphi(I) \frac{u_{k+1}^I - u_k^I}{\Delta t} + \frac{2}{c_2^2} \left(\varphi, \frac{u_{k+1} - 2u_k + u_{k-1}}{\Delta t^2}\right) \\ \qquad\qquad + a(\varphi, u_{k+1} + u_k) = 2\, (\varphi, F_k) \end{cases}$$

DOI: 10.1685/journal.caim.438

for $k = 0, \cdots, N_{\Delta t} - 1$, with $u_{-1} = u_0 = 0$.

Now, multiplying the first equation by p_k^I, inserting in the second equation $\varphi = u_{k+1} - u_k$ and summing up the two equations, we get:

$$2J_k^I + \tfrac{2}{c_2^2}\,(u_{k+1} - u_k, \tfrac{u_{k+1}-2u_k+u_{k-1}}{\Delta t^2}) + a(u_{k+1} - u_k, u_{k+1} + u_k) = 2\,(u_{k+1} - u_k, F_k) \tag{34}$$

where

$$J_k^I := \frac{1}{2}\Big[\frac{c_1 \Delta t}{E_1 A_1 E_2 A_2}(p_k^I)^2 + \frac{E_1 A_1 \Delta t}{E_2 A_2 c_1}(\frac{u_{k+1}^I - u_k^I}{\Delta t})^2\Big]\,. \tag{35}$$

Observing that it holds:

$$2\,(u_{k+1} - u_k, \frac{u_{k+1} - 2u_k + u_{k-1}}{\Delta t^2}) \geq |\frac{u_{k+1} - u_k}{\Delta t}|^2 - |\frac{u_k - u_{k-1}}{\Delta t}|^2 \tag{36}$$

and introducing the discrete energy

$$\mathcal{E}^{k+1} := \frac{1}{2}\Big[\frac{1}{c_2^2}|\frac{u_{k+1} - u_k}{\Delta t}|^2_{L^2(\Omega_2)} + \|u_{k+1}\|^2\Big]\,, \tag{37}$$

where $\|u\|^2 = a(u,u)$, from the previous equation one obtains the inequality:

$$J_k^I + \mathcal{E}^{k+1} - \mathcal{E}^k \leq (u_{k+1} - u_k, F_k) \tag{38}$$

from which:

$$\mathcal{E}^{k+1} - \mathcal{E}^k + J_k^I \leq \Delta t\, \mathcal{E}^{k+1} + \frac{\Delta t}{2}\,|c_2 F_k|^2\,. \tag{39}$$

Summing up for $k = 0, \cdots, n-1, \quad n \leq N_{\Delta t}$, we derive

$$\mathcal{E}^n + \sum_{k=0}^{n-1} J_k^I \leq\ \Delta t \sum_{k=0}^{n} \mathcal{E}^k + \frac{\Delta t}{2}\sum_{k=0}^{n-1}|c_2 F_k|^2\,. \tag{40}$$

Noting that $\sum_{k=0}^{n-1} J_k^I \geq 0$, it holds

$$\mathcal{E}^n \leq \Delta t\, \mathcal{E}^n + \Delta t \sum_{k=0}^{n-1} \mathcal{E}^k + \frac{\Delta t}{2}\sum_{k=0}^{n-1}|c_2 F_k|^2\,, \tag{41}$$

from which, under the coarse condition $\Delta t < 1$, we obtain

$$\mathcal{E}^n \leq \frac{\Delta t}{1 - \Delta t}\sum_{k=0}^{n-1} \mathcal{E}^k + \frac{\Delta t}{2(1 - \Delta t)}\sum_{k=0}^{n-1}|c_2 F_k|^2\,. \tag{42}$$

At last, applying the discrete Gronwall's Lemma [14] , we get a stability estimate for the FEM part of the numerical scheme:

$$\mathcal{E}^n \leq \frac{\Delta t}{2(1-\Delta t)} \sum_{k=0}^{n-1} |c_2 F_k|^2 \exp\left(\frac{n\Delta t}{1-\Delta t}\right). \tag{43}$$

Analogously, for the BEM part of the numerical scheme from (40) we get:

$$\sum_{k=0}^{n-1} J_k^I \leq \Delta t \sum_{k=0}^{n} \mathcal{E}^k + \frac{\Delta t}{2} \sum_{k=0}^{n-1} |c_2 F_k|^2 . \tag{44}$$

6. Numerical results.

In this first benchmark, taken from [12], we analyze a rod of unitary length, fixed in the left end-point and subjected to a uniform traction at the other end-point, i.e. $\bar{p}_2(t) = H(t)$. The forcing term on the second portion of the rod has been chosen $f_2(x,t) \equiv 0$. We consider a subdivision of the rod in two equal parts having: $A_1 = A_2 = 1$, $E_1 = E_2 = 1$, the same velocity of propagation: $c_1 = c_2 = 1$ and, of course, $L_1 = L_2 = 0.5$. The observation time interval is $(0, 10)$. For the discretization, we have used different temporal and spatial steps.
In Figures 1 and 2 we show numerical results obtained with $\Delta t = 0.01$, $\Delta x = 0.01$ and $\Delta t = 0.005$, $\Delta x = 0.005$: in particular, the time history of tractions at the left endpoint and at the interface and the time history of displacements in the right end-point and at the interface. The approximate solution improves refining the discretization parameters and it tends to the well known analytical solution [15].
Further, we have doubled the time interval of analysis to verify the stability of the proposed energetic approach: results are presented in Figure 3; they can be compared with those obtained in [12] with an energetic BEM-BEM coupling approach with $\Delta t = 0.1$, that are reported in Figure 4 for the reader's convenience: the high accuracy obtained by this approach is due to the fact that at each time step one has to solve a very little linear system with only four unknowns; besides, the chosen shape functions in time belong to the functional space of the boundary integral problem solution. The worse accuracy of the BEM-FEM approach is therefore mainly due to the FEM approximation: in Figure 5 we show the numerical results obtained, at the right end-pont of the rod and at the interface, with a pure energetic FEM approach with $\Delta t = 0.01, \Delta x = 0.01$. Always in this respect, we show in Figures 6 and 7 the numerical results obtained by the BEM-FEM coupling with the same discretization parameters but with two different

DOI: 10.1685/journal.caim.438

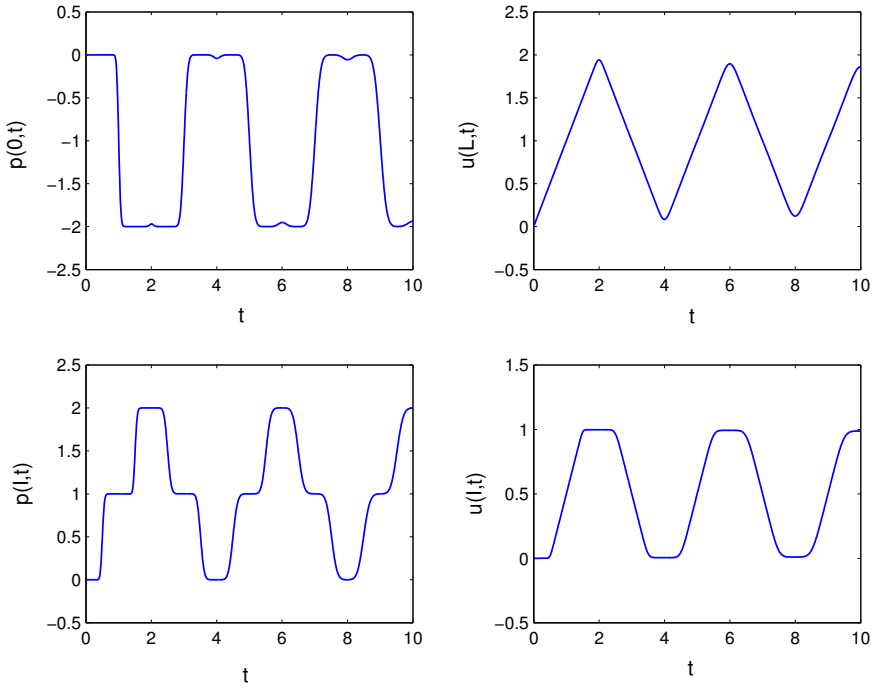

Figure 1. Numerical solution for the first benchmark, obtained with $\Delta t = 0.01, \Delta x = 0.01$.

decompositions of the rod, with lengths, respectively, $L_1 = 0.9, L_2 = 0.1$ and $L_1 = 0.99, L_2 = 0.01$: the smaller is the size of the second portion of the rod, i.e. of the FEM subdomain, the better is the numerical approximation of the solution.

In the second benchmark, treated in [12,15] with BEM-BEM coupling approaches, we consider a rod of length L consisting of two parts having the same material properties, as in the previous test. But while till now we have treated dimensionless problems, here we consider the following constants: length of each portion: $L_1 = L_2 = 5\,m$, transversal section area: $A_1 = A_2 = 10^{-4}\,m^2$, Young modulus: $E_1 = E_2 = 2.1\,10^8\,kN/m^2$, density: $\rho_1 = \rho_2 = 7.85\,t/m^3$ and therefore wave velocity: $c_1 = c_2 = 5172\,m/s$. The analysis is carried out until $T = 0.025\,s$. The rod is fixed in one end-point and subjected to a Heaviside load $\bar{p}_2(t) = -21\,kN\,H(t)$ applied at the other end-point. Here, $f_2(x,t) \equiv 0$.
In Figure 8 we present the approximate solution obtained by the energetic Galerkin BEM-FEM for $\Delta t = 5\,10^{-5}\,s\,, \Delta x = 0.25\,m$. Note that the time $length\,(\Omega_i)/c_i$, employed by the wave to travel from one end-point of Ω_i to

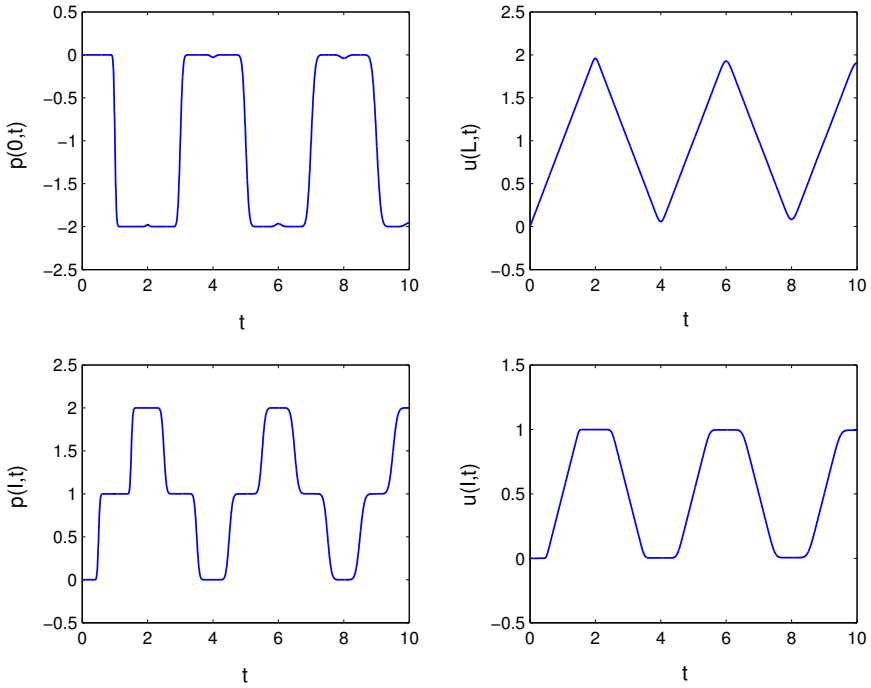

Figure 2. Numerical solution for the first benchmark, obtained with $\Delta t = 0.005$, $\Delta x = 0.005$.

the other, is not a multiple of the chosen time step Δt, but the numerical procedure remains stable.

The third benchmark involves an infinite rod, subdivided in two parts, $\Omega_1 = [1, +\infty)$, $\Omega_2 = [0, 1]$, with constants $E_1 = E_2 = 1$, $A_1 = A_2 = 1$ and $c_1 = c_2 = 1$. At the end-point $x = 0$ of the bounded portion, the rod is subjected to the Neumann datum $\bar{p}_2(t) = 3\,t^2$ and the forcing term on Ω_2 has been chosen as

$$f_2(x,t) = 6\,t^2(1-x) - 2(1-x)^3.$$

A Sommerfeld radiation condition is satisfied by displacement at infinity. This problem has solution given by

$$u(x,t) = \begin{cases} u_2(x,t) = t^2(1-x)^3, & 0 \le x \le 1 \\ u_1(x,t) = 0, & x > 1 \end{cases}.$$

The time interval of analysis is $[0, 5]$. In the following we show the numerical results obtained by the energetic Galerkin BEM-FEM approach with $\Delta t = 10^{-2}$, $\Delta x = 10^{-2}$. In Figure 9 we show the time history of the approximate

DOI: 10.1685/journal.caim.438

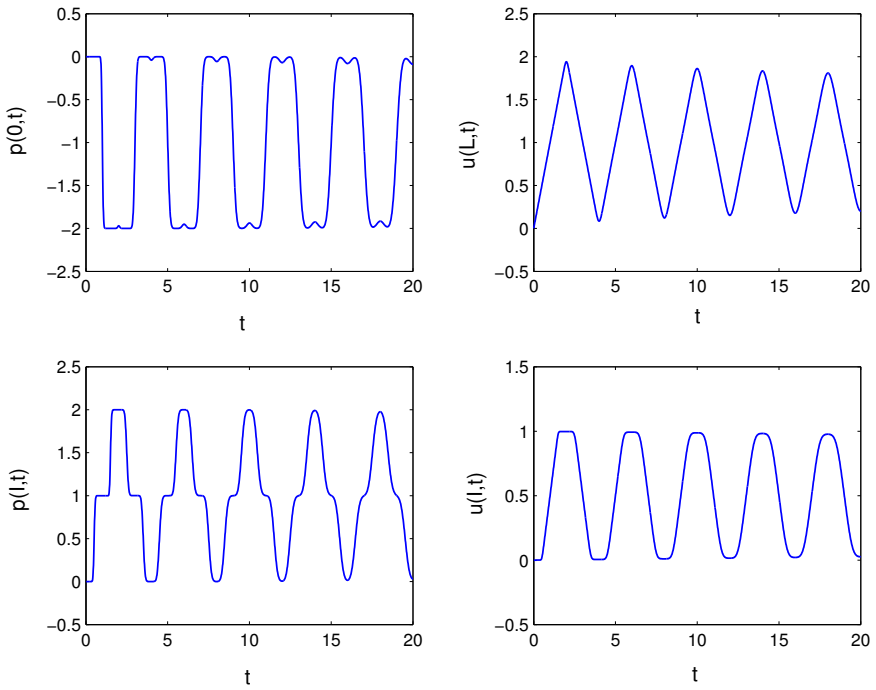

Figure 3. Numerical solution for the first benchmark, obtained with $\Delta t = 0.01, \Delta x = 0.01$, on a doubled time interval of analysis.

solution in $x = 0, \frac{1}{2}, 1$ (on the left) and of the absolute error in the same points in logarithmic scale (on the right). Note that along the whole time interval of analysis, it remains smaller than the order of magnitude of the discretization parameters. The same happens for the absolute error in the remaining nodes of the spatial mesh. In Figure 10 we show some snapshots of the approximate solution on the FEM subdomain Ω_2, at time instants $t = 0, 1, 2, 3, 4, 5$.

The last benchmark, taken again from [12,15], is related to a rod consisting of two parts, the first of them extending to infinity. These parts have different material properties and the corresponding constants are: $L_1 = \infty$, $L_2 = 5\,m$, $A_1 = A_2 = 10^{-4}\,m^2$, $E_1 = 2.1\,10^8\,kN/m^2$, $E_2 = 0.8\,10^8\,kN/m^2$, $\rho_1 = \rho_2 = 7.85\,t/m^3$; as a consequence $c_1 = 5172\,m/s$, $c_2 = 3192\,m/s$. The analysis is carried out until $T = 0.015\,s$. The rod is loaded at the end-point of the bounded portion with a rectangular impulse starting at time $t_0 = 0.001\,s$ and ending at time instant $t_1 = t_0 + 0.001\,s$, i.e. $\bar{p}_2(t) = 21\,kN\,(H(t - 10^{-3}) - H(t - 2\,10^{-3}))$. A Sommerfeld radiation con-

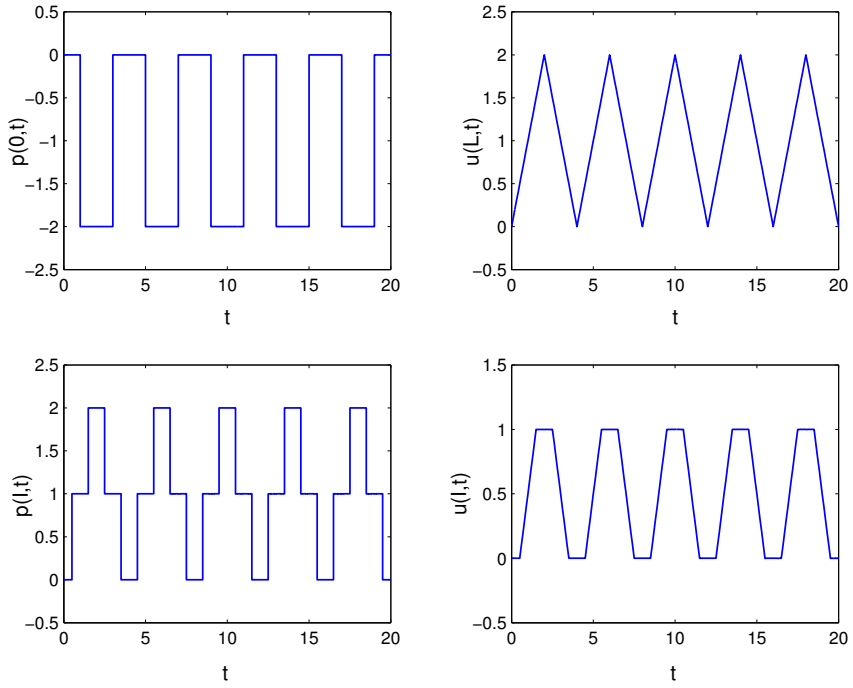

Figure 4. Numerical solution for the first benchmark, obtained with an energetic BEM-BEM coupling, with $\Delta t = 0.1$.

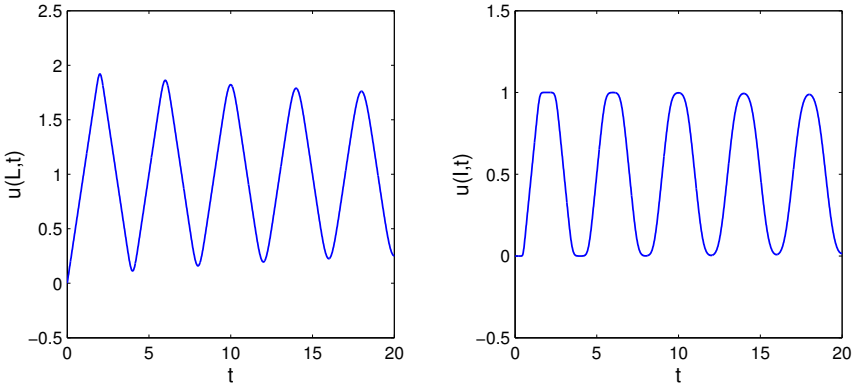

Figure 5. Numerical solution for the first benchmark, obtained with a pure energetic FEM approach, with $\Delta t = 0.01, \Delta x = 0.01$.

dition is satisfied by displacement at infinity. No forcing term is applied on Ω_2. For the discretization, we have used $\Delta t = 5.\,10^{-5}\,s\,, \Delta x = 0.05\,m$. In Figures 11 and 12 we show respectively the interface traction and the loaded end-point displacement, obtained by the energetic BEM-FEM cou-

DOI: 10.1685/journal.caim.438

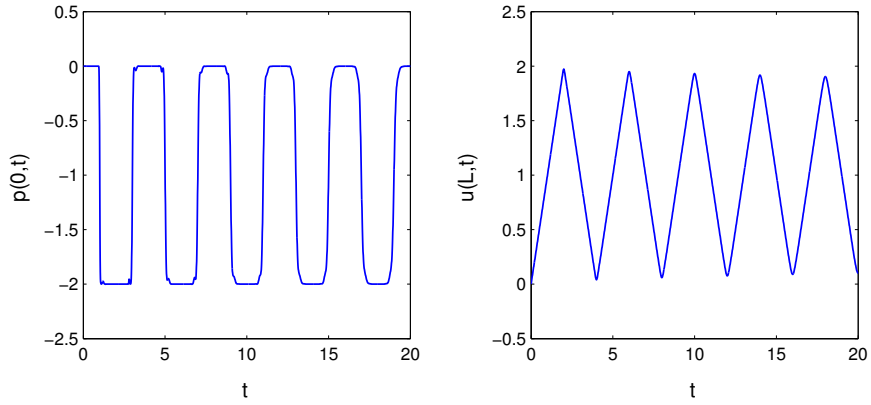

Figure 6. Numerical solution for $L_1 = 0.9, L_2 = 0.1$, obtained with $\Delta t = 0.01, \Delta x = 0.01$.

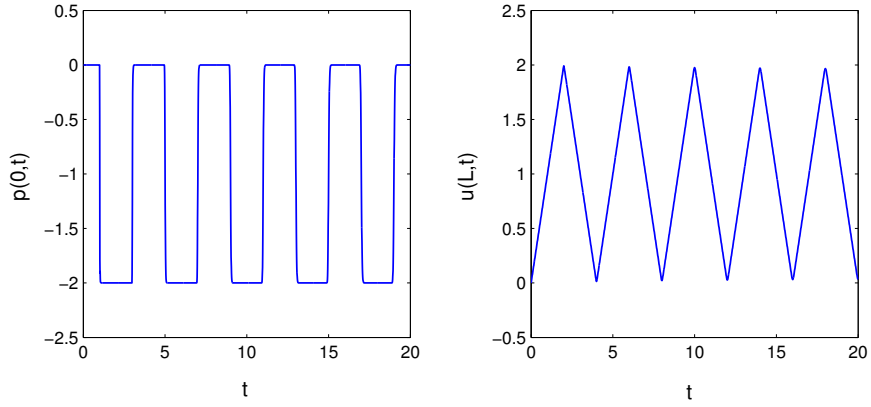

Figure 7. Numerical solution for $L_1 = 0.99, L_2 = 0.01$, obtained with $\Delta t = 0.01, \Delta x = 0.01$.

pling: our numerical results perfectly agree with those reported in [12] and are better than those presented in [15], especially for what concerns the approximate traction, which avoids spurious oscillations near the "jumps" of the solution, as instead it happens in the cited reference.

7. Conclusions.

In this paper, we have extended the energetic approach, recently introduced in the context of Galerkin BEM for wave propagation problems, in order to deal with efficient coupling BEM with FEM for bounded or unbounded multilayered media. First numerical results involving 1D wave propagation benchmarks have been presents and discussed. They appear

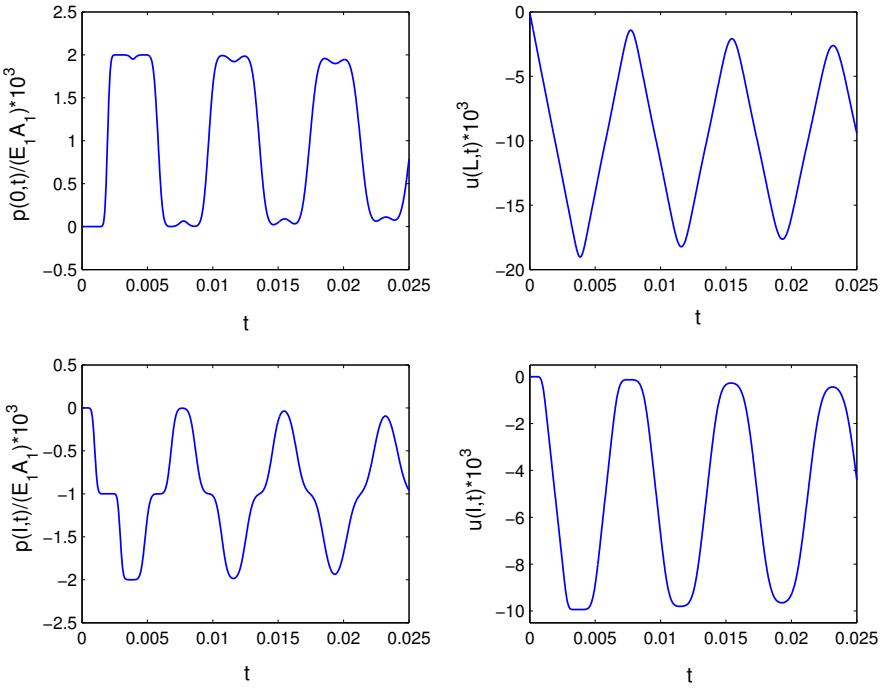

Figure 8. Numerical solution of the second benchmark, obtained with energetic BEM-FEM coupling, with $\Delta t = 5\,10^{-5}\,\mathrm{s}\,, \Delta x = 0.25\,\mathrm{m}$.

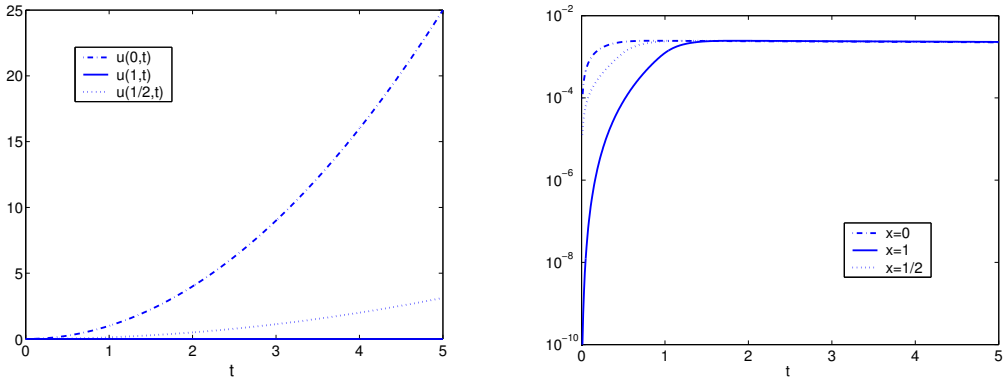

Figure 9. Time history of the approximate solution in $x = 0, \frac{1}{2}, 1$ (left) and of the absolute error in the same points (right), for the third test problem.

very promising; hence, we are actually focusing on the energetic BEM-FEM coupling for 2D and 3D model problems.

DOI: 10.1685/journal.caim.438

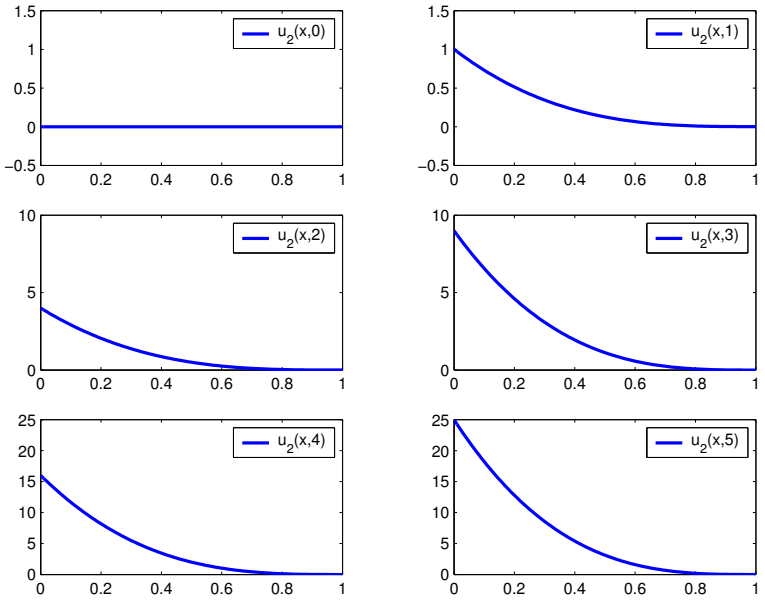

Figure 10. Snapshots of the approximate solution on the FEM subdomain Ω_2, at time instants $t = 0, 1, 2, 3, 4, 5$, for the third test problem.

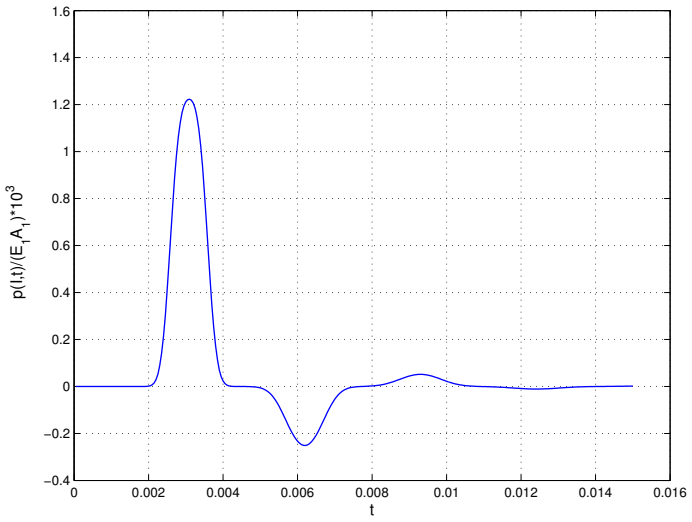

Figure 11. Time history of traction at the interface for the last benchmark.

REFERENCES

1. H. Antes, G. Beer, and W. Moser, Soil-structure interaction and wave propagation problems in 2D by a Duhamel integral based approach

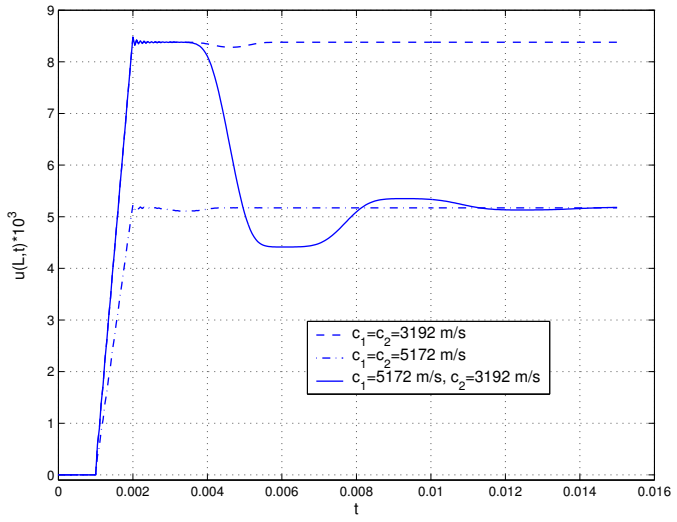

Figure 12. Time history of displacement at the loaded end-point for the last benchmark.

and the convolution quadrature method, *Comput. Mech.*, vol. 36, no. 6, pp. 431–443, 2005.

2. T. Ha Duong, B. Ludwig, and I. Terrasse, A Galerkin BEM for transient acoustic scattering by an absorbing obstacle, *Int. J. Num. Meth. Engrg.*, vol. 57, pp. 1845–1882, 2003.
3. A. Buffa, M. Costabel, and C. Schwab, Boundary element methods for Maxwell's equations on non-smooth domains, *Numer. Math.*, vol. 92, no. 4, pp. 679–710, 2002.
4. M. Sari and I. Demir, Wave modelling through layered media using the BEM, *Journal of Applied Sciences*, vol. 6, no. 8, pp. 1703–1711, 2006.
5. V. S. Almeida and J. B. Paiva, Static analysis of soil/pile interaction in layered soil by BEM/BEM coupling, *Advances in Engineering Software*, vol. 38, pp. 835–845, 2007.
6. O. Czygan and O. von Estorff, Fluid-structure interaction by coupling BEM and nonlinear FEM, *Engineering Analysis with Boundary Elements*, vol. 26, pp. 773–779, 2002.
7. J. L. Wegner, M. M. Yao, and X. Zhang, Dynamic wave-soil-structure interaction analysis in the time domain, *Computers & Structures*, vol. 83, pp. 2206–2214, 2005.
8. W. J. Mansur, G. Yu, J. A. M. Carrer, S. T. Lie, and E. F. N. Siqueira, The θ scheme for time-domain BEM/FEM coupling applied to the 2-D scalar wave equation, *Comm. Numer. Methods Engrg.*, vol. 16, no. 6, pp. 439–448, 2000.

DOI: 10.1685/journal.caim.438

9. S. T. Lie and G. Y. Yu, Stability improvement to BEM/FEM coupling scheme for 2D scalar wave problems, *Advances in Engineering Software*, vol. 33, pp. 17–26, 2002.
10. G. Y. Yu, A symmetric BEM/FEM coupling procedure for 2-D elastodynamic problems, *Journal of Applied Mechanics*, vol. 70, pp. 451–454, 2003.
11. T. Abboud, P. Joly, J. Rodriguez, and I. Terrasse, Coupling discontinuous Galerkin methods and retarded potentials for transient wave propagation on unbounded domains, *J. Comput. Physics*, vol. 230, no. 15, pp. 5877–5907, 2011.
12. A. Aimi and M. Diligenti, A new space-time energetic formulation for wave propagation analysis in layered media by BEMs, *Int. J. for Num. Meth. in Eng.*, vol. 75, no. 9, pp. 1102–1127, 2008.
13. A. Aimi, S. Gazzola, and C. Guardasoni, Energetic boundary element method analysis of wave propagation in 2D multilayered media, *Methods in the Applied Sciences*, vol. 35, pp. 1140–1160, 2012.
14. A. Quarteroni and A. Valli, *Numerical Approximation of Partial Differential Equations*. Springer-Verlag, 1994.
15. W. Moser, H. Antes, and G. Beer, A Duhamel integral based approach to one-dimensional wave propagation analysis in layered media, *Comput. Mech.*, vol. 35, pp. 115–126, 2005.